Aging of Cholinesterases Phosphylated by Tabun Proceeds through O-Dealkylation

ARTICLE *in* JOURNAL OF THE AMERICAN CHEMICAL SOCIETY · DECEMBER 2008

Impact Factor: 12.11 · DOI: 10.1021/ja804941z · Source: PubMed

J|A|C|S
ARTICLES

Published on Web 11/01/2008

Aging of Cholinesterases Phosphylated by Tabun Proceeds through O-Dealkylation

Eugénie Carletti,[†] He Li,[‡] Bin Li,[‡] Fredrik Ekström,[§] Yvain Nicolet,[#] Mélanie Loiodice,[†] Emilie Gillon,[†] Marie T. Froment,[†] Oksana Lockridge,[‡] Lawrence M. Schopfer,[‡] Patrick Masson,[†] and Florian Nachon*[,†]

Département de Toxicologie, Centre de Recherches du Service de Santé des Armées (CRSSA), 24 avenue des Maquis du Grésivaudan, 38700 La Tronche, France, Eppley Institute and Department of Biochemistry and Molecular Biology, University of Nebraska Medical Center, Omaha, Nebraska 68198-6805, FOI CBRN Defence and Security, S-901 82 Umeå, Sweden, and Laboratoire de Cristallogenèse et Cristallographie des Protéines, Institut de Biologie Structurale (CEA-CNRS-UJF), 41 rue Jules Horowitz, 38027 Grenoble, France

Received June 27, 2008; E-mail: fnachon@crssa.net

Abstract: Human butyrylcholinesterase (hBChE) hydrolyzes or scavenges a wide range of toxic esters, including heroin, cocaine, carbamate pesticides, organophosphorus pesticides, and nerve agents. Organophosphates (OPs) exert their acute toxicity through inhibition of acetylcholinesterase (AChE) by phosphylation of the catalytic serine. Phosphylated cholinesterase (ChE) can undergo a spontaneous, time-dependent process called "aging", during which the OP−ChE conjugate is dealkylated. This leads to irreversible inhibition of the enzyme. The inhibition of ChEs by tabun and the subsequent aging reaction are of particular interest, because tabun−ChE conjugates display an extraordinary resistance toward most current oxime reactivators. We investigated the structural basis of oxime resistance for phosphoramidated ChE conjugates by determining the crystal structures of the non-aged and aged forms of hBChE inhibited by tabun, and by updating the refinement of non-aged and aged tabun-inhibited mouse AChE (mAChE). Structures for non-aged and aged tabun−hBChE were refined to 2.3 and 2.1 Å, respectively. The refined structures of aged ChE conjugates clearly show that the aging reaction proceeds through O-dealkylation of the P(*R*) enantiomer of tabun. After dealkylation, the negatively charged oxygen forms a strong salt bridge with protonated His438Nϵ2 that prevents reactivation. Mass spectrometric analysis of the aged tabun-inhibited hBChE showed that both the dimethylamine and ethoxy side chains were missing from the phosphorus. Loss of the ethoxy is consistent with the crystallography results. Loss of the dimethylamine is consistent with acid-catalyzed deamidation during the preparation of the aged adduct for mass spectrometry. The reported 3D data will help in the design of new oximes capable of reactivating tabun−ChE conjugates.

Introduction

Acetylcholinesterase (AChE; EC 3.1.1.7) and butyrylcholinesterase (BChE; EC 3.1.1.8) are closely related serine hydrolases with different substrate specificities and inhibitor sensitivities. AChE terminates the action of the neurotransmitter acetylcholine at postsynaptic membranes and neuromuscular junctions. Although BChE is present in numerous vertebrate tissues, its physiological role remains unclear.[1,2]

Human butyrylcholinesterase (hBChE) is toxicologically relevant because it hydrolyzes or scavenges a wide range of toxic esters, including heroin, cocaine, carbamate pesticides, organophosphorus pesticides, and nerve agents.[3] Organophosphates (OPs) exert their acute toxicity through inhibition of AChE by phosphylation of the catalytic serine. Subsequent accumulation of acetylcholine at neuronal synapses and neuromuscular junctions results in paralysis, seizures, and other symptoms of cholinergic syndrome.[4,5]

Phosphylated ChEs can be reactivated by nucleophilic agents such as oximes. The most effective oximes used for emergency treatment of nerve agent poisoning are the monopyridinium oximes (2-PAM and HI-6) and bispyridinium oximes (TMB-4, MMB-4, obidoxime, and HLö-7).[6] Kinetic analysis of the interactions between different AChE-OP conjugates and different oximes shows that the most effective oximes are HLö-7 for phosphonylated AChE and obidoxime for phosphorylated AChE.[6] Unfortunately, a universal antidote, efficient against all known nerve agents and capable of crossing the blood−brain barrier, is not yet available.

Subsequent to formation of the OP−ChE adduct, the phosphylated ChEs can undergo a spontaneous, time-dependent

[†] Département de Toxicologie, CRSSA.
[‡] University of Nebraska Medical Center.
[§] FOI CBRN Defence and Security.
[#] Institut de Biologie Structurale.

(1) Chatonnet, A.; Lockridge, O. *Biochem. J.* **1989**, *260*, 625–634.
(2) Mack, A.; Robitzki, A. *Prog. Neurobiol.* **2000**, *60*, 607–628.
(3) Lockridge, O.; Masson, P. *Neurotoxicology* **2000**, *21*, 113–126.
(4) Eddleston, M.; Mohamed, F.; Davies, J. O.; Eyer, P.; Worek, F.; Sheriff, M. H.; Buckley, N. A. *Qjm* **2006**, *99*, 513–522.
(5) Konradsen, F.; Dawson, A. H.; Eddleston, M.; Gunnell, D. *Lancet* **2007**, *369*, 169–170.
(6) Worek, F.; Thiermann, H.; Szinicz, L.; Eyer, P. *Biochem. Pharmacol.* **2004**, *68*, 2237–2248.

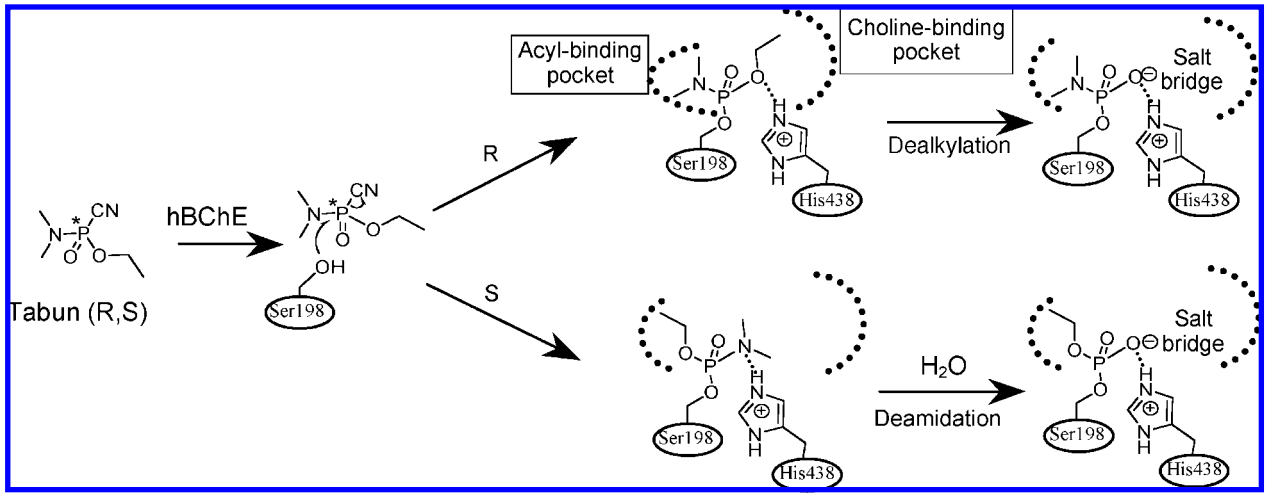

Figure 1. Mechanism proposed for aging of hBChE phosphorylated by tabun.

process called "aging", during which the OP−ChE conjugate is dealkylated. This leads to irreversibly inhibited enzyme.[7−10] The rate of aging depends on the nature of the OP. The $t_{1/2}$ is a few minutes for ChE inhibited by soman[11] and several hours for ChE inhibited by tabun.[12]

Early studies showed that tabun-inhibited ChEs from different animals display different rates of aging.[13] The rate constant for aging of tabun-inhibited human AChE (hAChE) *in vitro* was found to be 8.7×10^{-4} min^{-1} (i.e., $t_{1/2}$ =13.3 h) at 37° and pH 7.4.[12]

Inhibition of ChEs by tabun and the subsequent aging reaction are of particular interest, because tabun−ChE conjugates display an extraordinary resistance toward most oxime reactivators. As tabun is racemic, the two enantiomers, P(*R*) and P(*S*), can react with the enzyme and form adducts with different stereochemistry. These adducts could respectively age through "dealkylation" or "deamination" (Figure 1).

Mass spectrometry (MS) studies on the aging of hAChE inhibited by tabun suggested that the mechanism involved a P−N bond cleavage and elimination of the dimethylamine group.[14,15] Intriguingly, the 2.5 Å crystal structure of non-aged *Mus musculus* AChE (mAChE) inhibited by tabun suggested that the ethoxy moiety is placed close to the catalytic His447, with the dimethylamine group distant from catalytic residues able to facilitate the aging reaction.[16] In the structure, the His447 and Phe338 side chains have undergone a structural change relative to the conformation found in the apoenzyme structure. The authors proposed that this displacement might interfere with the accessibility of oximes, thereby contributing to the high resistance of tabun conjugates to reactivators.

Kinetic analysis of the oxime-induced reactivation and aging of hAChE inhibited by various tabun-related *N*-monoalkyl phosphoramidates showed that the rate constants for both were dependent on the length of the *N*-alkyl chain.[17]

In order to better understand the structural basis of both the oxime resistance of the conjugates and the aging mechanism of tabun-inhibited ChEs, we analyzed peptides from tabun−hBChE by MS, determined the crystal structures of non-aged and aged forms of hBChE inhibited by tabun, and updated the previous crystal structure model of tabun−mAChE. The X-ray structures will help in the design of new oximes capable of reactivating tabun−ChEs conjugates.

Materials and Methods

Caution: *As tabun is highly toxic and is classified as a schedule 1 chemical as defined in the Chemical Weapons Convention, all work with tabun is regulated by the convention. The handling of tabun is dangerous and requires suitable personal protection, training, and facilities.*

Titration of Tabun by Ionometry and NMR. Racemic tabun in solution in 2-propanol was from CEB (Vert-le-Petit, France). ^{31}P, ^{1}H, and ^{13}C NMR spectra for tabun in 2-propanol were recorded to determine its purity and integrity. After complete hydrolysis at pH 13.6, tabun was titrated by ionometry using a thermostatted ionometer (Radiometer IONcheck 45) equipped with an ion-selective electrode for cyanide (Radiometer Analytical ISE25CN-9), as described by the electrode provider.

Production of Recombinant hBChE. The recombinant hBChE was a truncated monomer containing residues 1−529.[18] The 45-amino acid tetramerization domain at the carboxy terminus was deleted. The carbohydrate content was reduced by site-directed mutagenesis from nine to six glycans.[18] The recombinant hBChE gene was expressed in Chinese hamster ovary (CHO) cells. The enzyme, secreted into serum-free culture medium, was purified by affinity and ion-exchange chromatographies and crystallized as

(7) Benschop, H. P.; Keijer, J. H. *Biochim. Biophys. Acta* **1966**, *128*, 586–588.
(8) Viragh, C.; Kovach, I. M.; Pannell, L. *Biochemistry* **1999**, *38*, 9557–9561.
(9) Millard, C. B.; Kryger, G.; Ordentlich, A.; Greenblatt, H. M.; Harel, M.; Raves, M. L.; Segall, Y.; Barak, D.; Shafferman, A.; Silman, I.; Sussman, J. L. *Biochemistry* **1999**, *38*, 7032–7039.
(10) Nachon, F.; Asojo, O. A.; Borgstahl, G. E.; Masson, P.; Lockridge, O. *Biochemistry* **2005**, *44*, 1154–1162.
(11) Saxena, A.; Viragh, C.; Frazier, D. S.; Kovach, I. M.; Maxwell, D. M.; Lockridge, O.; Doctor, B. P. *Biochemistry* **1998**, *37*, 15086–15096.
(12) Heilbronn, E. *Biochem. Pharmacol.* **1963**, *12*, 25–36.
(13) Heilbronn, E. *Biochim. Biophys. Acta* **1962**, *58*, 222–230.
(14) Barak, D.; Ordentlich, A.; Kaplan, D.; Barak, R.; Mizrahi, D.; Kronman, C.; Segall, Y.; Velan, B.; Shafferman, A. *Biochemistry* **2000**, *39*, 1156–1161.
(15) Elhanany, E.; Ordentlich, A.; Dgany, O.; Kaplan, D.; Segall, Y.; Barak, R.; Velan, B.; Shafferman, A. *Chem. Res. Toxicol.* **2001**, *14*, 912–918.
(16) Ekstrom, F.; Akfur, C.; Tunemalm, A. K.; Lundberg, S. *Biochemistry* **2006**, *45*, 74–81.
(17) Worek, F.; Aurbek, N.; Koller, M.; Becker, C.; Eyer, P.; Thiermann, H. *Biochem. Pharmacol.* **2007**, *73*, 1807–1817.
(18) Nachon, F.; Nicolet, Y.; Viguié, N.; Masson, P.; Fontecilla-Camps, J. C.; Lockridge, O. *Eur. J. Biochem.* **2002**, *269*, 630–637.

described.[18] The active-site concentration of highly purified enzyme was determined using diisopropyl fluorophosphate as the titrant.[19]

Production of Recombinant hAChE. The recombinant L544Stop mutant of human AChE (monomeric) was inserted into a pGS vector carrying the glutamine synthetase gene marker. CHO-K1 cells were maintained in serum-free Ultraculture Medium (Bio-Whittaker). Cells were transfected using DNA−calcium phosphate precipitation. Transfected clones were selected by incubation in media containing methionine sulfoximide. When cell death subsided, individual clones were manually transferred to 24 well plates. Clones with high expression of AChE were expanded and transferred to roller bottles for large-scale protein production. The used growth media contained up to 30 mg of hAChE per liter. Protein was precipitated from the media by ammonium sulfate. The pellets were dialyzed against 20 mM Tris-HCl buffer, pH 7.4, and loaded onto an affinity column (Sepharose-4B/procainamide). Human AChE was eluted with 20 mM Tris-HCl buffer, pH 7.4, containing 1 M NaCl, 0.5 M tetramethylammonium iodide, and 1 mM decamethonium chloride. The enzyme was dialyzed against 20 mM Tris-HCl buffer, pH 7.4, and further purified by ion-exchange chromatography (monoQ; Amersham Bioscience) on a fast protein liquid chromatography system (Pharmacia). Fractions containing high hAChE activity were pooled and concentrated using a Centricon-30 ultrafiltration microconcentrator (30 000 MW cutoff, from Amicon). The concentration of the pure, homogeneous hAChE was determined from its absorbance at 280 nm using $\epsilon_{1\ \mathrm{mg/mL}} = 1.7$.[20]

Inhibition of hChEs by Tabun. Phosphylation rates were determined by incubating the ChE with different concentrations of tabun in 50 mM sodium phosphate buffer, pH 7.0, containing 5% 2-propanol and 1 mg/mL bovine serum albumin (BSA) and measuring the enzyme residual activity of aliquots at various times after initiation of inhibition at 25 °C. Human ChE activities were assayed according to Ellman[21] with 1 mM butyrylthiocholine for hBChE and 0.75 mM acetylthiocholine (ATC) for hAChE in the presence of 1 mg/mL BSA, 0.5 mM 5,5′-dithiobis(2-nitrobenzoic-acid), and 50 mM sodium phosphate buffer, pH 7.0, at 25 °C using a Uvikon943 spectrophotometer. The stability of tabun under the assay conditions was verified by ionometry (measurement of CN^- release) and by testing the invariant ability of tabun solution to inhibit hBChE as a function of time. No significant spontaneous hydrolysis of tabun was observed after more than 10 h of incubation. Analysis of the kinetic data was performed using GOSA-fit, a fitting software based on a simulated annealing algorithm (BioLog, Toulouse, France; http://www.bio-log.biz).

Cholinesterases are well-known to favor one stereoisomer over another. Therefore, it is prudent to analyze the tabun inhibition kinetics as if the ChE were behaving in a stereoselective manner. The rate of dissociation of the ChE−tabun adduct is slow relative to its rate of formation; therefore, the phosphylation reaction can be treated as an irreversible process for analytical purposes.

Irreversible inhibition by a racemic inhibitor (*R*,*S*) can be described by Scheme 1. The apparent bimolecular phosphylation rate constants ($k_i = k_{iR} + k_{iS}$, see Scheme 1) determined under pseudo-first-order conditions ([tabun] > 20[hChE]) were computed from the slopes of ln *E* vs time plots at different tabun concentrations.

Determination of inhibition enantioselectivity was performed under second-order conditions. The concentration of hBChE was 31.5 nM, while that of tabun ranged between 25 and 200 nM. The concentration of hAChE was 7.4 nM, while that of tabun ranged between 5 and 150 nM. Assuming that the enzymes were enantioselective, with one enantiomer much more efficient than the other (i.e, $k_{iR} \gg k_{iS}$), the fraction of enzyme inhibited by the lowest active

Scheme 1[a]

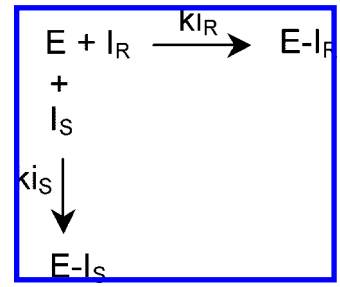

[a] E is the enzyme, I_R is the *R* enantiomer, I_S is the *S* enantiomer, E-I_R and E-I_S are the conjugates, and k_{iR} and k_{iS} are the bimolecular rate constants.

enantiomer is negligible, and the concentration of residual active enzyme follows eq 1 (derived from Scheme 1) as a function of time:

$$E = E_0 \frac{E_0 - I_0/n}{E_0 - (I_0/n)\, e^{(I_0/n - E_0)k_{iR}t}} \quad (1)$$

where *E* is the concentration of residual active enzyme at time *t*, E_0 the concentration of enzyme at time $t = 0$, I_0 the concentration of racemic inhibitor at $t = 0$, *n* the number of enantiomers, and k_{iR} the bimolecular rate constant of the most active enantiomer (taken to be enantiomer *R* in this case).

Tabun-Inhibited hBChE Samples for Mass Spectrometry. Human BChE was reacted with tabun in $H_2{}^{18}O$. Oxygen-18 was used so that the mechanism of dealkylation during aging could be more clearly defined. Evidence from the crystal structure of aged tabun-inhibited hBChE indicates that aging involves dealkylation of the ethoxy moiety. This reaction requires hydrolysis of the P−O−C linkage. In principle, such a hydrolysis could occur by cleavage of the P−O bond or the O−C bond. In the former case, a hydroxyl from water would replace the ethoxy. In the latter case, a hydroxyl from water would add to the ethyl, leaving the original oxygen on the phosphorus. By using $H_2{}^{18}O$, the site of cleavage can be distinguished. If hydrolysis is at the O−C bond, the mass of the phosphorus component will reflect the presence of the original ^{16}O. If the hydrolysis is at the P−O bond, the phosphorus component will gain an ^{18}O from the medium and its mass will increase by 2 amu. This strategy was employed by Li et al. to characterize the aging reactions for a variety of hBChE−OP adducts.[22]

For the inhibition reaction, 10 μL of recombinant hBChE (13 mg/mL in 15 mM 2-(*N*-morpholino)ethanesulfonic acid (MES) buffer at pH 6.5) was mixed with 90 mL of $H_2{}^{18}O$, 1 mL of 1 M Tris buffer at pH 8.5, and 1 mL of tabun (10 mg/mL in 2-propanol). Samples for analysis of the non-aged adduct were frozen to −80 °C shortly after preparation. Samples for analysis of the aged adduct were incubated at room temperature for 2 days, after which the preparation was stored at −80 °C until use. Final concentrations of hBChE and tabun were 15 and 720 mM, respectively. Unlabeled hBChE was treated in the same manner, except that the tabun was omitted.

To prepare peptides for MS, frozen samples were thawed and 50 mL of sample was mixed with 50 mL of 25 mM ammonium bicarbonate buffer at pH 8.3. The mixture was concentrated to about 20 mL by centrifugation at 6700*g* using a Microcon YM-3 ultrafiltration microconcentrator (3000 MW cutoff, from Millipore). The process was repeated five times to remove the $H_2{}^{18}O$ and excess tabun and to change the buffer. The product was diluted to 50 mL with 25 mM ammonium bicarbonate, mixed with porcine trypsin (0.5 mg/mL from Promega) to a final hBChE/trypsin ratio of 30:1 (w/w), and incubated overnight at room temperature with constant,

(19) Amitai, G.; Moorad, D.; Adani, R.; Doctor, B. P. *Biochem. Pharmacol.* **1998**, *56*, 293–299.
(20) Rosenberry, T. L.; Scoggin, D. M. *J. Biol. Chem.* **1984**, *259*, 5643–5652.
(21) Ellman, G. L.; Courtney, K. D.; Andres, V.; Featherstone, R. M. *Biochem. Pharmacol.* **1961**, *7*, 88–95.
(22) Li, H.; Schopfer, L. M.; Nachon, F.; Froment, M. T.; Masson, P.; Lockridge, O. *Toxicol. Sci.* **2007**, *100*, 136–145.

gentle mixing. Peptides were concentrated and washed using ZipTips (Millipore), as described in the sections on MALDI-TOF mass spectrometry and Q-Trap mass spectrometry.

MALDI-TOF Mass Spectrometry. MALDI-TOF MS experiments were performed on an Applied Biosystems Voyager DE-PRO mass spectrometer equipped with a 337 nm pulsed nitrogen laser (Framingham, MA). Peptides that had been adsorbed onto a reverse-phase C-18 ZipTip were eluted into a microcentrifuge tube with 15 μL of 60% acetonitrile and 0.1% trifluoroacetic acid (TFA). One microliter of eluant was mixed 1:1 (v/v) with α-cyano-4-hydroxycinnamic acid (matrix, 10 mg/mL in 50% acetonitrile and 0.3% TFA) on the MALDI target plate and allowed to dry at room temperature. Mass spectra were acquired in positive-ion, linear mode under delayed extraction conditions, using an acceleration voltage of 20 kV. Laser intensity was adjusted so that the most intense ion in the spectrum did not exceed 80% of the maximum, saturated intensity value. Laser positioning on the sample spot was monitored with a video camera. Spectra shown are the average of 500 laser shots collected from multiple locations on the target spot. Calibration for the mass spectra was performed internally by reference to hBChE tryptic fragments. The sequence of hBChE (accession no. gi:158429457) was obtained from the NCBInr database. The reference masses of the tryptic hBChE peptides were obtained using the MS-Digest feature of ProteinProspector version 4.0.6 (http://prospector.ucsf.edu/).

Q-Trap Mass Spectrometry. The amino acid sequence of the aged peptide from tabun-inhibited hBChE was determined by collision-induced dissociation in a QTrap 2000, hybrid, tandem-quadrupole, linear-ion trap mass spectrometer equipped with a nanospray interface (Applied Biosystems). The spectrometer was calibrated daily on selected fragments from the MSMS spectrum of [Glu]fibrinopeptide B. Tryptic peptides from tabun-inhibited hBChE (25 μL total volume) were subjected to ZipTip cleanup to remove salts before they were delivered into the QTrap. Ten microliters of an 80% acetonitrile and 0.1% formic acid solution was used to elute the peptides from the ZipTip. Two 25-μL aliquots were cleaned and the eluents combined. Eight microliters of the peptide solution was introduced into the mass spectrometer by static infusion using an Econo12 emitter (New Objective, Woburn, MA). The ion spray voltage was 1300 V (which creates a voltage differential of 1300 V between the emitter and the curtain plate). The emitter position was optimized to obtain maximum signal intensity. All mass spectra were collected in the enhanced mode, i.e., using the ion trap, and by convention are referred to as enhanced spectra. Enhanced product ion (EPI) spectra were obtained using low-energy collision-induced dissociation. The collision cell was pressurized to 40 μTorr with pure nitrogen. The collision energy was 40 V. The trap fill time for each EPI scan was 20 ms. A total of 200 EPI scans were accumulated to generate the final EPI spectrum. The EPI spectra were manually analyzed to determine the sequence of the peptide.

Crystals of Non-aged Tabun-Inhibited hBChE Conjugate. The mother liquor was 0.1 M MES buffer, pH 6.5, with 2.1 M ammonium sulfate. The tabun stock solution was 10 mM in 2-propanol. The tabun−hBChE conjugate was prepared by soaking crystals for 10 min in 0.1 M MES buffer, pH 6.5, with 2.1 M ammonium sulfate containing 1 mM tabun. The crystals were washed with a cryoprotectant solution (0.1 M MES buffer with 2.1 M ammonium sulfate, containing 20% glycerol) and then flash-cooled in liquid nitrogen.

Crystallization of Aged Tabun−hBChE Conjugate. The purified enzyme (9 mg/mL) was inhibited in the presence of 1 mM tabun in 10 mM Tris-HCl buffer, pH 7.4. The reaction mixture was incubated for 1 day at 4 °C. The inhibited enzyme was crystallized using the hanging drop method as described.[23] Crystals grew in 1 week at 20 °C. The length of time between phosphylation and data collection was sufficiently long (>1 week) to achieve completion of the aging reaction.

X-ray Data Collection and Structure Solution of Tabun−hBChE Conjugate. Diffraction data were collected at the European Synchrotron Radiation Facility (ESRF, Grenoble, France), at the ID14-eh2 beam line using $\lambda = 0.932$ Å wavelength with ADSC Quantum 4 for non-aged conjugate, and at the ID23-2 beam line using $\lambda = 0.873$ Å wavelength with MAR-Research CCD detector for aged conjugate. All data sets were processed with XDS. The structures were solved by use of the CCP4 suite.[24] An initial solution model was determined by molecular replacement with MolRep,[25] starting from the recombinant hBChE structure (PDB entry 1P0I) from which all ligands (butyrate, glycerol, ions) and glycan chains were removed. For all diffraction data sets, the model was refined as follows: an initial rigid-body refinement with REFMAC5[26] was followed by iterative cycles of model building with Coot,[27] and then restrained refinement was carried out with REFMAC5 and Phenix.[28] The bound ligands and their descriptions were built using the Dundee PRODRG2.5 server including energy minimization using GROMOS96.1 force field.

Updated Refinement of Aged and Non-aged Tabun-Inhibited mAChE. Coordinates and structure factors of non-aged (PDB entry 2C0Q) and aged (PDB entry 2C0P) tabun-inhibited mouse AChE were retrieved from the Protein Data Bank. The models were refined by iterative cycles of model building with Coot and restrained refinement with REFMAC5 and Phenix.

Results

Inhibition of Human Cholinesterases by Tabun. The bimolecular rate constants, k_i, for inhibition of hAChE and hBChE by racemic tabun are respectively $(3.0 \pm 0.4) \times 10^6$ and $(2.0 \pm 0.2) \times 10^6$ $M^{-1}\cdot min^{-1}$ (data not shown). These values are in agreement with reported literature values.[29]

The time dependence of the inhibition of hAChE and hBChE by tabun, under second-order conditions, is shown in Figure 2. Both human ChEs are enantioselective. Fitting the AChE data to eq 1 yields $k_{iR} = (6.9 \pm 0.2) \times 10^6$ $M^{-1}\cdot min^{-1}$ and $n = 2.1 \pm 0.1$. This corresponds to enantioselectivity of hAChE for one enantiomer of tabun. For hBChE, fitting yields $k_{iR} = (6.0 \pm 0.4) \times 10^6$ $M^{-1}\cdot min^{-1}$ and $n = 2.7 \pm 0.1$. The latter n value also suggests an enantioselectivity of hBChE. However, the fact that more than 2 equiv of tabun was required to achieve full enzyme inhibition is puzzling. The value $n = 2.7$ was systematically found for inhibition of both highly purified tetrameric plasma BChE and monomeric recombinant BChE. Because both tabun and BChE preparations were accurately titrated, and because no spontaneous hydrolysis of tabun was observed in buffer, a tentative hypothesis is that hydrolysis of tabun was promoted by a BChE nucleophile group other than Ser198. This requires further investigations.

Mass Spectrometry Analysis of Tabun−hBChE Adducts. The initial reaction of hBChE with tabun is expected to result in formation of a covalent adduct with loss of the CN moiety from tabun. This would cause the mass of the singly charged, active-

(23) Nicolet, Y.; Lockridge, O.; Masson, P.; Fontecilla-Camps, J. C.; Nachon, F. *J. Biol. Chem.* **2003**, *278*, 41141–41147.

(24) Collaborative-Computational-Project 4. *Acta Crystallogr. D, Biol. Crystallogr.* **1994**, *50*, 760−763.

(25) Vagin, A.; Teplyakov, A. *J. Appl. Crystallogr.* **1997**, *30*, 1022–1025.

(26) Murshudov, G. N.; Vagin, A. A.; Dodson, E. J. *Acta Crystallogr. D, Biol. Crystallogr.* **1997**, *53*, 240–255.

(27) Emsley, P.; Cowtan, K. *Acta Crystallogr. D, Biol. Crystallogr.* **2004**, *60*, 2126–2132.

(28) Adams, P. D.; Grosse-Kunstleve, R. W.; Hung, L. W.; Ioerger, T. R.; McCoy, A. J.; Moriarty, N. W.; Read, R. J.; Sacchettini, J. C.; Sauter, N. K.; Terwilliger, T. C. *Acta Crystallogr. D, Biol. Crystallogr.* **2002**, *58*, 1948–1954.

(29) Raveh, L.; Grunwald, J.; Marcus, D.; Papier, Y.; Cohen, E.; Ashani, Y. *Biochem. Pharmacol.* **1993**, *45*, 2465–2474.

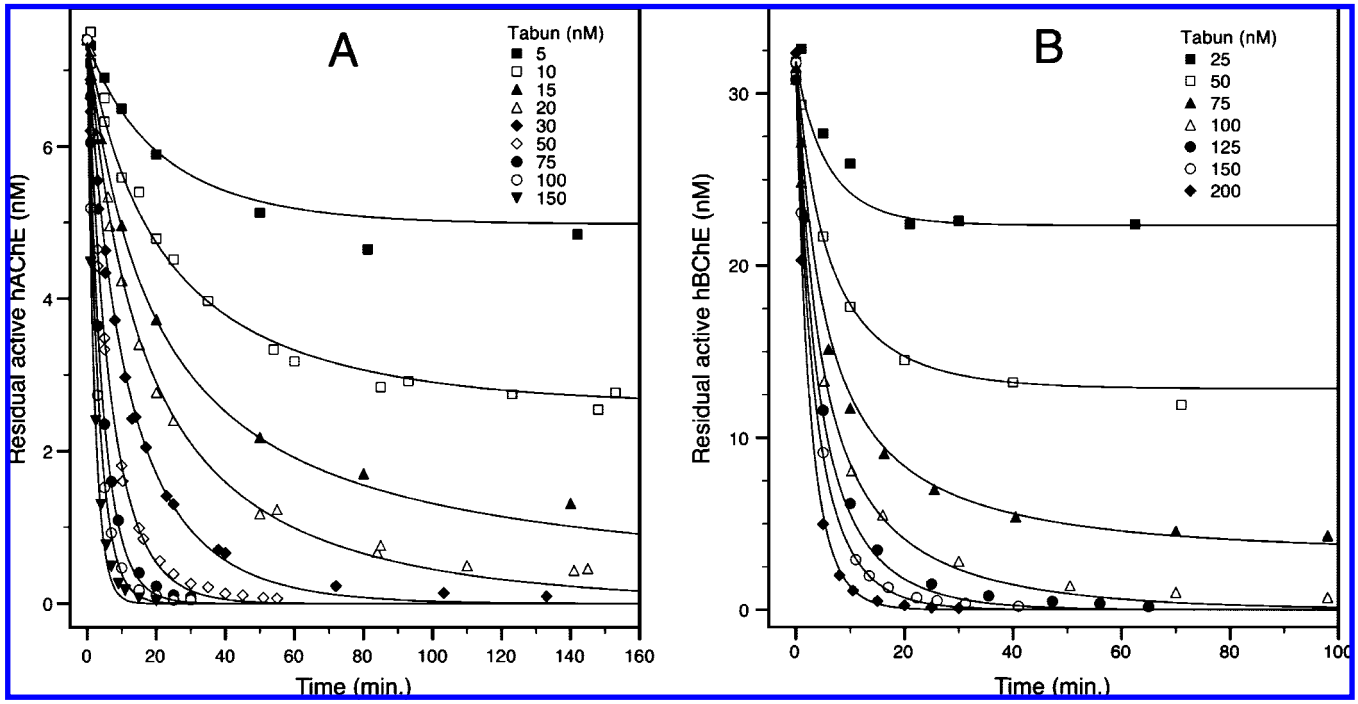

Figure 2. Irreversible inhibition of hAChE (A) and hBChE (B) by racemic tabun under second-order conditions. Human ChEs were inhibited by various concentrations of tabun, and the residual active concentration of enzyme was monitored as a function of time.

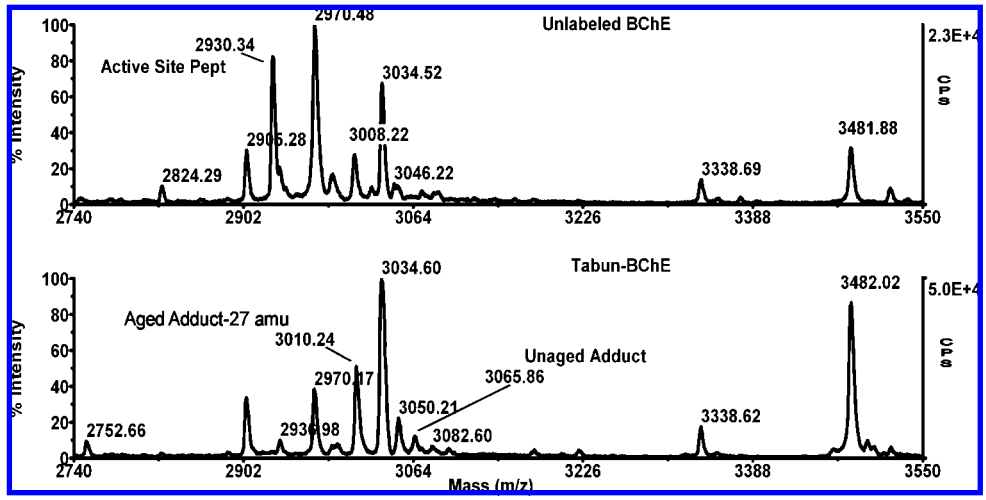

Figure 3. Mass spectra of tryptic digests of hBChE with and without tabun. Spectra were taken in linear mode on a MALDI-TOF mass spectrometer. Peptides were prepared and MALDI-TOF mass spectra were taken as described in the methods section. The upper panel is for unlabeled hBChE. It was internally calibrated using the average masses for hBChE peptides at 3482.07 (residues 148−180) and 3034.59 amu (residues 428−452). The lower panel is for the aged tabun−hBChE adduct. The peak labeled "Aged Adduct-27 amu" is the peak for tabun−hBChE after loss of the dimethylamine and ethoxy groups. It was internally calibrated using the hBChE peptides at 3482.07 (residues 148−180), 3050.59 (residues 428−452 with one oxidized methionine), and 3034.59 amu (residues 428−452). Calibration was performed using peak height as a weighting factor.

site, tryptic peptide to increase by 135 amu, from 2930.3 to 3065.3 amu (average masses). This transformation is evident in the MALDI-TOF mass spectra shown in Figure 3, where the tryptic digest of unlabeled hBChE (upper panel) shows a prominent peak at 2930.34 amu and no mass at 3065 amu, while the tryptic digest of the non-aged tabun−hBChE adduct (lower panel) shows no mass at 2930 amu and a distinct mass at 3065.86 amu.

Following its initial formation, the tabun−hBChE adduct will age. Aging would be expected to result in loss of either a dimethylamine or an ethoxy group. Such losses would lead to reduction in the mass of the active-site peptide adduct to either 3038.3 (for loss of dimethylamine) or 3037.3 amu (for loss of ethoxy). Neither of these masses was detected in the MALDI-TOF mass spectra for the aged tabun−hBChE adduct. The large peak at 3034 amu (from hBChE peptide residues 428−452) could obscure peaks of small intensity at 3037 or 3038 amu. However, high-resolution, reflector-mode MALDI-TOF spectra showed that the peak at 3034 amu (average mass) was composed only of isotopes from a 3032 amu monoisotopic mass. There was no evidence in the isotopic pattern for additional mass at 3037 or 3038 amu. This finding was unexpected since the tabun−hBChE adduct had been allowed to age for several days before digestion and aged product should have been present.

Comparison of the two mass spectra in Figure 3 reveals a shift in the mass of the 3008 amu peak in unlabeled hBChE to

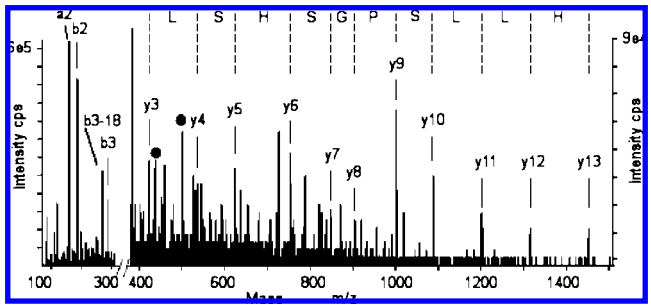

Figure 4. Tandem mass spectrum (MSMS) of the putative aged tabun-labeled active-site peptide from hBChE. An MSMS spectrum was taken of the 753.4 *m/z*, quadruply charged form of the 3010 amu ion using the QTrap 2000 hybrid tandem-quadrupole, linear ion-trap mass spectrometer. The *x*-axis is divided into two intensity ranges. For masses from 400 to 1500 *m/z*, the intensity of the data has been expanded 6.7-fold. The intensities for this region are given in counts per second (cps) on the scale to the right. For masses from 50 to 350 *m/z*, the intensities are given in cps on the scale to the left. Selected y- and b-ions that are characteristic of hBChE active-site peptide are indicated. The amino acid sequence corresponding to the y-ion series is indicated by single-letter abbreviations for the amino acids. The spots indicate the 437.3 and 501.4 amu fragments; see the text for a description of these fragments.

3010 amu in the aged tabun−hBChE sample. The 3008 amu mass is consistent with the mass of a tryptic peptide from hBChE (residues 549−570 having one oxidized methionine). The 3010 amu mass appeared repeatedly in the spectra of aged tabun−hBChE. A mass of 3010 amu would be consistent with loss of both the dimethylamine and the ethoxy groups from the tabun adduct, leaving phosphate (added mass of 80 amu) attached to the active-site peptide.

Justification for the loss of both substituents can be made. The crystallography results indicate that the ethoxy group is lost through the aging process. Hydrolysis of dimethylamine from tabun is known to occur at low pH.[30] During preparation of peptides for positive-mode MALDI-TOF mass spectrometry, samples were routinely exposed to 0.1% TFA. Thus, loss of the dimethylamine could occur. The combination would have resulted in reduction of the tabun adduct to a phosphate adduct.

Confirmation of the identity of the 3010 amu mass was obtained by tandem mass spectrometry. Tryptic peptides from hBChE were infused into a QTrap 2000 tandem-quadrupole mass spectrometer. A mass equal to the quadruply charged form of the 3010 amu ion was observed at 753.4 *m/z*. This mass was subjected to collision-induced dissociation in the mass spectrometer. The resulting MSMS mass spectrum was consistent with that of the active-site peptide from hBChE (Figure 4).

The sequence of the active-site peptide is SVTLFGE**S**AGAASVSLHLLSPGSHSLFTR, where the bold-type S at position 8 is the serine that is expected to be labeled. A singly charged, y-ion series identical to the C-terminal portion of the active-site peptide, HLLSPGSHSL(FTR), was clearly defined in the MSMS spectrum. Singly charged fragments from the N-terminal were also found (a2 at 159.1 amu for SV minus CO, b2 at 187.2 amu for SV, b3 at 288.1 amu for SVT, and b3 minus water at 270.1 amu). Most convincing, however, were two doubly charged masses, at 437.3 and 501.4 *m/z*, which are consistent with phosphoserine fragments $b9^{2+}$ (SVTLFGE**S**A) and $b11^{2+}$ (SVTLFGE**S**AGA) that have lost 98 amu. Both fragments include the labeled serine. Loss of 98 amu from a phosphoserine is a commonly observed consequence of collision-induced dissociation. It represents loss of the phosphate (−80 amu) and transformation of the serine into dehydroalanine (−18 amu).

Thus, both the MALDI-TOF and tandem mass spectrometry results are consistent with the presence of a phosphoserine-containing, active-site peptide in the aged form of tabun-labeled hBChE. The most logical scenario to explain this species is loss of the ethoxy ligand through aging and loss of the dimethylamine ligand through acid-catalyzed hydrolysis during preparation of the sample for mass spectrometry. Only evidence of deamination was found in earlier mass spectrometry studies on human AChE.[14,15] This suggests that only the product of the acid-catalyzed deamination could be observed under those experimental conditions.

This analysis of aged tabun−hBChE utilizes an added mass of 80 amu for phosphate, which is the mass expected if natural abundance oxygen-16 is present for all of the oxygens on the phosphorus. If aging had involved release of the dimethylamine, then one of the phosphorus oxygens should have been derived from the $H_2{}^{18}O$ in the medium, making the added mass of the phosphate 82 amu. Similarly, if aging involved release of the ethoxy moiety via P−O bond cleavage, then the added mass would have been 82 amu. It follows that the added mass is consistent with elimination of the ethoxy moiety during aging via O−C bond cleavage.

X-ray Structure of Non-aged Tabun-Inhibited hBChE. Data were collected from tetragonal crystals of space group *I*422 and refined to 2.1 Å. Data and refinement statistics are shown in Table 1. There is no significant displacement of residue side chains compared to the native enzyme (PDB entry 1P0I). A strong peak of positive electronic density (19σ) within covalent bond distance of the catalytic serine was observed in the initial $|F_o| - |F_c|$ map. This confirms that inhibitor was bound to the active-site serine after 5 min of soaking. The structure was refined as a conjugate of the P(*R*) enantiomer of tabun (Figure 5A). The phosphorus atom is found at covalent bonding distance of 1.65 Å from the Ser198Oγ atom. O2 of the phosphoramidate moiety is at hydrogen-bonding distance from the main-chain amide nitrogen of residues forming the oxyanion hole, Gly116 (2.9 Å), Gly117 (2.8 Å), and Ala199 (2.9 Å). The ethoxy moiety is pointing toward the top of the active-site gorge, with O3 at hydrogen-bonding distance from His438Nϵ2 (3.2 Å). The dimethylamino moiety is located in the acyl-binding pocket with the two methyl groups pointing toward the top of the gorge. Despite the fact that the P−N distance was refined to 1.8 Å, there is still a residual peak of positive density (4σ) above the two methyl groups. This density could correspond to low occupancy of the butyrate-like molecule that is always found in the native enzyme structure.[23] The C1 methyl group of the dimethylamine is interacting with Leu286Cδ2 and Phe398CZ (both at 3.5 Å) and the C2 methyl group is at 3.2 Å from Gly117Cα and 3.8 Å from Trp231Cϵ3. There is a peak of positive density in the initial $|F_o| - |F_c|$ map (5.4σ) close to Trp82 that could not be reasonably modeled. A similarly shaped density was found in the choline-binding pocket in several structures of native hBChE. In those structures, it was modeled as glycerol (1P0I or 1XLV).[10,23] This unknown ligand appears to be stacked against Trp82 and seems to interact with Glu197Oϵ2, a water molecule from the cluster along Trp430 and Tyr440, and the water molecule H-bonded to Thr120.

X-ray Structure of Aged Tabun-Inhibited hBChE. Data were collected from a crystal of aged tabun-inhibited hBChE and were refined to 2.3 Å. A strong peak of positive electronic density

(30) Larsson, L. *Acta Chim Scand* **1958**, *12*, 783–785.

Table 1. Data Collection and Refinement Statistics

	tabun−hBChE		tabun−mAChE	
	non-aged (3DJY)	aged (3DKK)	non-aged (3DL4)	aged (3DL7)
space group	*I*422	*I*422	*P*212121	*P*212121
unit cell axes, *a*, *b*, *c* (Å)	156.58, 127.74	155.24, 127.47	79.62, 112.94, 226.16	79.02, 110.88, 226.38
no. of measured reflections	305 954	236 247	n.d.[d]	n.d.[d]
unique reflections	45 888	34 165	71 021	69 074
resolution (Å)	55.4−2.1 (2.2−2.1)	28.2−2.3 (2.4−2.3)	29.2−2.5 (2.6−2.5)	29.0−2.5 (2.6−2.5)
completeness (%)	99.0 (99.6)	98.2 (93.0)	99.6 (100.0)	99.3 (99.0)
R_{merge}[a] (%)	6.3 (50.5)	6.6 (42.7)	9.0 (59.0)	7.0 (51.0)
$I/\sigma(I)$	22.0 (4.4)	27.6 (5.1)	14.4 (3.3)	17.6 (7.5)
redundancy	6.7 (7.0)	6.9 (7.3)	6.2 (6.2)	7.4 (7.5)
Refinement Statistics				
R-factor[b] (*R*-free[c])	21.2 (24.8)	19.6 (24.6)	19.6 (24.5)	18.8 (22.7)
no. of atoms				
protein	4213	4192	8444	8403
solvent	285	275	133	439
others	154	154	168	72
mean *B*-factor (Å^2)	39.8	40.1	47.2	49.6
rms from ideality				
bond length (Å)	0.017	0.022	0.014	0.013
angles (deg)	1.764	2.068	1.501	1.461
chiral (Å^3)	0.123	0.140	0.105	0.097

[a] $R_{merge} = (\sum|I - \langle I\rangle|)/\sum I$, where I is the observed intensity and $\langle I\rangle$ is the average intensity obtained from multiple observations of symmetry-related reflections after rejections. [b] *R*-factor $= \sum|F_o - |F_c||/\sum|F_o|$, where F_o and F_c are observed and calculated structure factors. [c] *R*-free set uses 5% of randomly chosen reflections defined by Brunger et al.[38] [d] Structure factors come from the PDB: 2C0Q (non-aged) and 2C0P (aged).

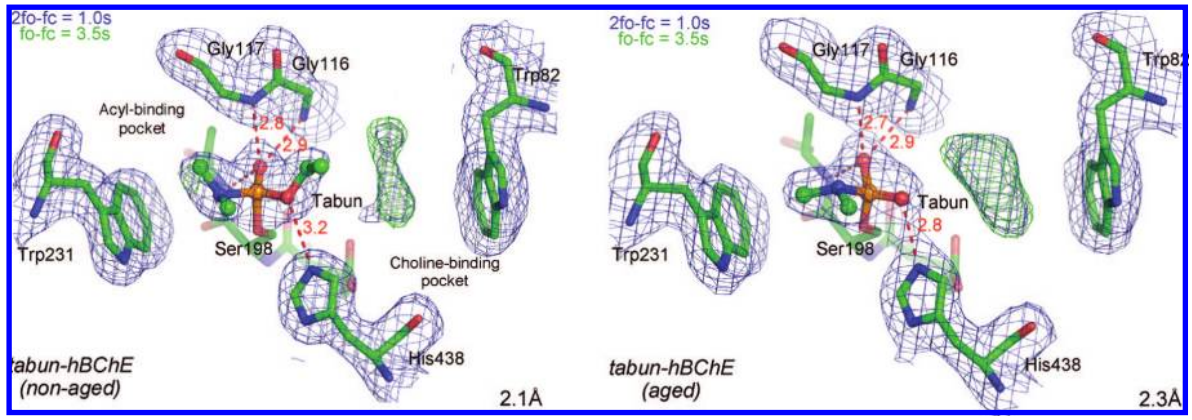

Figure 5. Active site of non-aged and aged tabun−hBChE conjugates. Key residues are represented as sticks with carbon atoms in green, nitrogen atoms in blue, phosphorus in orange, and oxygen atoms in red. Hydrogen bonds are represented by red dashes. Electron density $2|F_o| - |F_c|$ is represented by a blue mesh, contoured at 1.0σ, and $|F_o| - |F_c|$ is represented by green/red mesh contoured at 3.5σ.

(13σ) within covalent bond distance of the catalytic serine in the initial $|F_o| - |F_c|$ map confirms the presence of the bound inhibitor. The refined structure clearly shows that aging proceeds through O-dealkylation of the P(*R*) enantiomer of tabun (Figure 5B). The phosphorus atom is found at a covalent bonding distance of 1.62 Å from the Ser198Oγ atom. O2 of the phosphoramidate moiety is at hydrogen-bonding distance from the main-chain amide nitrogens of the residues forming the oxyanion hole, Gly116 (2.9 Å), Gly117 (2.7 Å), and Ala199 (2.7 Å). As a result of the loss of the ethoxy substituent, the O3 moiety of the phosphorus is negatively charged and forms a strong salt bridge with His438Nϵ2 (2.8 Å). The dimethylamino moiety is located in the acyl-binding pocket, but in contrast to the non-aged form, the two methyl groups point downward from Phe398. The C2 methyl group interacts with the indole ring of Trp231, about 3.5 Å from each aromatic carbon of the six-atom ring, while C1 is at least 3.7 Å from Phe398, Phe329, and Leu286. The P−N distance was refined to 1.7 Å. The peak of positive density that was close to Trp82 in the non-aged tabun−hBChE $|F_o| - |F_c|$ map is still present but is much stronger (9.1σ). It is likely that the occupancy of this ligand is higher because there is no steric hindrance from the ethoxy, and there is a possibility for stronger H-bond interactions with the negatively charged O3 of the phosphoramidate.

Updated Refinement of Non-aged Tabun-Inhibited mAChE. The original geometry of the aged and non-aged tabun moiety was based on calculations using the monomer library sketcher of the CCP4 program suite.[24] However, a careful examination of the crystal structure of non-aged tabun-inhibited mAChE reveals questionable geometry for the phosphoramidate adduct in both monomers (PDB code 2C0Q). For example, the N−P−Ser203Oγ angle was refined to 83°, which is at odds with the angle of 103° determined using the GROMOS96.1 force field analysis. The 103° value is in better agreement with the tetrahedral shape of the adduct. In addition, the P and N atoms and the two methyl groups were modeled as strictly coplanar, whereas molecular modeling based on GROMOS96.1 force field indicates an sp^3 orbital hybridization of N. However, quantum mechanics computation at the BP86/TZVP level indicates a hybridization of N between sp^2 and sp^3. This mixed hybridization is supported by two small-molecule structures in

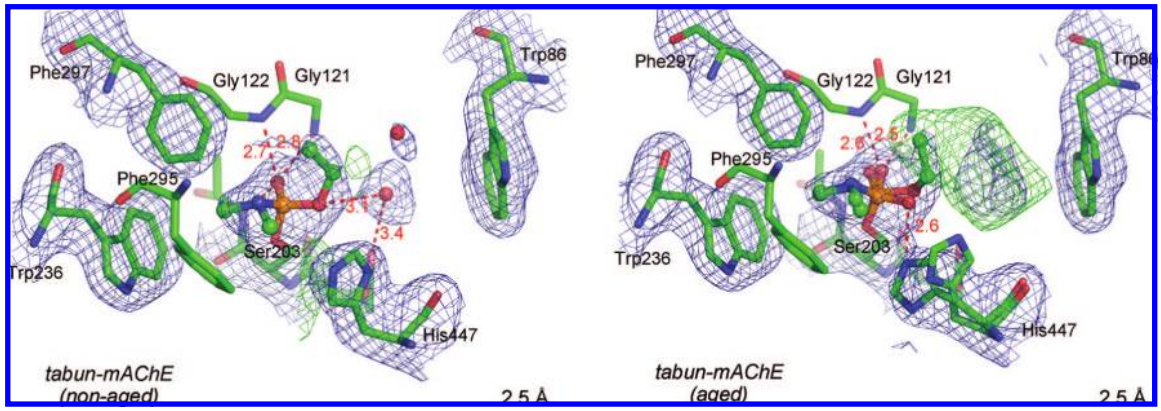

Figure 6. Active site of non-aged and aged tabun−mAChE conjugates. Key residues are represented as sticks, with carbon atoms in green, nitrogen atoms in dark blue, phosphorus in orange, and oxygen atoms in red. Hydrogen bonds are represented by red dashes. Electron density $2|F_o| - |F_c|$ is represented by a blue mesh, contoured at 1.0σ, and $|F_o| - |F|$ is represented by green/red mesh contoured at 3.5σ.

the Cambridge Structural Database (QOQWOI[31] and ZEXBAF[32]) in which dimethylamino groups are attached to phosphorus. Because of these ambiguities, a new refinement was made using better constraints for tabun (Figure 6A).

In the new refinement, the methyl groups of the dimethylamine are pointing downward, in a conformation similar to that found in aged tabun-inhibited hBChE. The C2 methyl group interacts with Trp236Cζ3 (3.5 Å) and Phe295Cϵ1, whereas C1 is 3.4 Å from Phe295Cζ. As previously reported, the imidazolium ring of His447 has shifted toward Phe338. There is a residual peak of density (4.5σ) in the $|F_o| - |F|$ map between Ser203 and Glu334 of both monomers that suggests some low-occupancy conformations of His447. Two water molecules were added to explain residual density close to Trp86 at the bottom of the gorge. The remainder of the gorge is apparently free of ligands. There is a noteworthy "blob" of density (up to 5.4σ) close to Trp286, which indicates that the peripheral anionic site is occupied by an unknown ligand (data not shown).

Updated Refinement of Aged Tabun-Inhibited mAChE. In the original refinement (PDB code 2C0P), the modeled tabun−mAChE adduct underwent aging through displacement of the dimethylamine moiety from the acyl-binding pocket, while the ethoxy substituent was left intact in the choline-binding pocket, pointing toward the top of the gorge. The actual electronic density shows that the dimethylamine group is still attached to the phosphorus atom. While there is clearly some electron density in the $2|F_o| - |F|$ map corresponding to an ethoxy substituent in monomer A, there appears to be none in monomer B. In addition, a peak of positive density next to His447 in both monomers suggests that His447 may adopt an alternate conformation. There were large "blobs" of unexplained density in the $|F_o| - |F|$ map stretching from the peripheral site (Trp286) to the choline-binding site (Trp86), hinting that the whole gorge is occupied by unknown ligands. This material has perturbed the conformation of Tyr337. On the basis of these observations, it was concluded that an improved model should be built.

For monomer A, the presence of electronic density in the choline binding site indicated that the aged conjugate underwent incomplete dealkylation. Accordingly, both aged and non-aged forms of the tabun conjugates were included in the new model. They were assigned an occupancy of 0.5 each, based on *B*-factor values, though a large uncertainty exists on this ratio (Figure 6B). The position and the array of interactions in the non-aged tabun adduct in monomer A are similar to those in the non-aged structure of mAChE. In the aged form, the phosphorus atom is found at a covalent bonding distance of 1.6 Å from the Ser203Oγ atom. O2 of the phosphoramidate moiety is at hydrogen-bonding distance from the main-chain amide nitrogens of the residues forming the oxyanion hole, Gly121 (2.8 Å), Gly122 (2.6 Å), and Ala204 (2.8 Å). The dimethylamino moiety is still located in the acyl-binding pocket, with the two methyl groups pointing downward. The C2 methyl group is interacting with the indole ring of Trp236, CH2 (3.5 Å), whereas C1 is 3.5 Å from Phe295Cζ and 3.3 Å from Phe338Cζ. The electron density of His447 is not clearly defined and was modeled as two conformers, despite features indicating that there is more likely a continuum of conformations between the two average positions. In the first conformer, His447Nϵ2 forms a salt bridge with O3 of the phosphorus (2.6 Å), and His447Nδ1 is strongly H-bonded to Glu334Oϵ1 (2.5 Å). The second conformer is similar to the conformation of the non-aged conjugate. These two models highlight the fact that dealkylation is accompanied by a shift of the phosphoramidate moiety toward His447Nϵ2 (0.7 Å shift for O3). In addition, nearby residues Tyr337 and Phe338 are extremely perturbed. Their side chains were refined to occupancies of 0.6 and 0.8, respectively. The perturbation of the Tyr337 conformation, in particular, appears to be related to the presence of an unknown ligand close to Trp86. This is indicated by the strong unexplained positive electron density in the $|F_o| - |F|$ map (peak at 8.8σ). We tried to fit this electron density to (1) components of the crystallization buffer, polyethylene glycol monomethyl ether 750, HEPES; and (2) procainamide, the ligand that was used for the last affinity chromatography purification step,[16] without success.

For monomer B, at first sight the weak electron density for the ethyl substituent suggested that complete dealkylation of the conjugate had occurred. However, it became apparent during the refinement process that the weak residual density was better explained by modeling both aged and non-aged forms of the tabun adduct into the structure. For example, when the adduct was modeled solely as the aged form, a peak of positive density in the $|F_o| - |F|$ map developed between His447Nϵ2 and O3. This indicated that the refinement software was placing O3 too far away from the imidazolium. This would arise if the software was trying to fit density corresponding to trace amounts

(31) Gholivand, K.; Tadjarodi, A.; Taeb, A.; Garivani, G.; Ng, S. W. *Acta Crystallogr.* **2001**, *E57*, o472–o473.
(32) Shih, Y.-E.; Wang, F.-C.; Maa, S.-H.; Liu, L.-K. *Bull. Inst. Chem. Acad. Sin.* **1994**, *41*, 9.

of the ethoxy substituent. Accordingly, models for both the aged and non-aged forms of the tabun adduct were refined into the structure with occupancies of 0.6 and 0.4, respectively. This ratio was based on a *B*-factor value of about 41 Å^2. The position and the array of interactions in the non-aged and aged tabun adducts are similar to those in monomer A: the two methyl groups point downward and make contacts with Trp236, Phe295, and Phe338, and there is a slight shift of the phosphoramidate toward His447NE2 (0.6 Å for O3). His447 is again perturbed and, consequently, is modeled as two alternate conformations displaying average positions like those in monomer A. Nearby residues, Phe338 and Tyr337, are extremely perturbed and were refined with partial occupancy. This perturbation, at least that of Tyr337, is related to the presence of an unknown ligand in the active site, which is indicated by strong positive peaks in the $|F_o| - |F|$ maps (7.2σ).

Discussion

The kinetics for inhibition of hBChE and hAChE by tabun show that both enzymes are enantioselective. This is in agreement with a previous study showing that (−)-tabun reacts about 6.3 times faster than (+)-tabun with electric eel AChE.[33] However, for hBChE and hAChE, the enantioselectivity may be larger than 1 order of magnitude.

Assuming in-line substitution, the X-ray structure of non-aged tabun−hBChE reveals that the enzyme is mainly inhibited by P(*R*)-tabun with the dimethylamine group located in the acyl-binding pocket. Stereoselectivity may result from preferred H-bonding of His438 to the ethoxy substituent and interaction of Trp231 with the dimethylamine moiety. The same considerations apply for the structure of non-aged tabun−mAChE,[16] the refinement of which was improved in the present study. The X-ray structure of aged tabun−hBChE also showed enantioselectivity for P(*R*)-tabun; i.e., the electron density shows that the dimethylamine moiety is located in the acyl-binding pocket. The same enantioselectivity was found in the updated refinements of aged tabun−mAChE and from the structure of aged tabun−TcAChE.[34] These observations provide structural evidence that there is a selectivity of cholinesterases for the P(*R*) enantiomer of tabun. This has important implications for the aging pathway. Combining the enantioselectivity results from the solution kinetics with those from the X-ray crystal structures suggests that (−)-tabun is P(*R*)-tabun.

The first X-ray structure of an aged tabun−cholinesterase was made with mouse AChE (PDB code 2C0P).[16] This structure was determined following 4 weeks of aging, which, with an aging half-time of a few hours, should have been sufficient to complete the reaction. Still, an incomplete dealkylation led to an adduct model with the ethoxy group present in the choline-binding pocket and the *N*-dimethyl group substituted by hydroxyl.

That model implied that aging occurs through nucleophilic attack by water on the P−N bond and subsequent scission of that bond. However, the conformation of the adduct in the active site was peculiar. First, the oxygen arising from loss of the dimethylamine was located in the acyl-binding pocket with no possibility for stabilization through formation of a salt bridge. Previous structural data for aged AChEs indicated that the phosphorus oxygen resulting from aging was stabilized by formation of a salt bridge with His447.[9,10,23,34,35] Second, there were no groups in the acyl pocket that could promote aging. It is generally accepted that the active site of cholinesterase accelerates the aging process. This acceleration is generally thought to involve the histidine from the catalytic triad and the tryptophan from the choline-binding pocket. If the aging process for tabun required similar assistance, the dimethylamine moiety would have been located in the choline-binding pocket. Since the de-dimethylamidated moiety was located in the acyl-binding pocket in the mAChE model, there would have been a rearrangement of the substituents around the phosphorus after aging. Such motions are doubtful in a constrained active-site pocket like that of mAChE. All of these factors suggest that the aged tabun−mAChE model requires refinement.

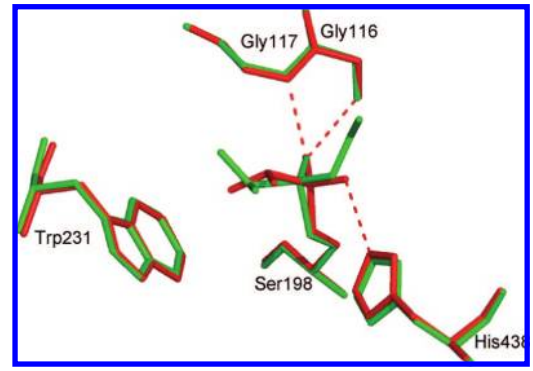

Figure 7. Superimposition of active sites of the non-aged (green) and aged (red) tabun−hBChE conjugates.

The new model for aged tabun−mAChE shows unambiguously that the ethoxy substituent underwent dealkylation. The X-ray structure of aged tabun−hBChE and the structure of aged tabun−TcAChE[34] both support this interpretation. The negatively charged phosphoryl oxygen that results from aging forms a salt bridge with the catalytic imidazolium in each case. There is no doubt that aging of these three phosphoramidated cholinesterases proceeds through the classic aging pathway worked out for phosphonylated human AChE.[10,22,35,36] In that mechanism, the imidazolium stabilizes a developing negative charge on the $C-O^{\delta-}$ oxygen, and a water molecule activated by Glu202 (197 in hBChE) attacks the carbocationic center that appears on the $C^{\delta+}-O$ carbon, thus leading to scission of the C−O bond, release of the alkoxy moiety, and subsequent formation of the salt bridge between the phosphorus O3-oxygen and the imidazolium.

This mechanism can be extended to tabun−hAChE via the following logical argument. Knowing that (1) dealkylation of tabun−ChE conjugates occurs in three different ChEs, (2) residues lining the active-site gorge of mAChE and hAChE are identical, and (3) hAChE is enantioselective for tabun stereoisomers, we can reasonably state that aging of tabun−hAChE proceeds through dealkylation of the ethoxy substituent.

The formation of the salt bridge between the phosphorus O3-oxygen and the imidazolium of His438 in aged tabun−hBChE induces a small rearrangement of the phosphoramidyl-serine, while the active-site residues, notably His438, do not move (Figure 7). His438 is stabilized by a strong hydrogen bond with

(33) Degenhardt, C.; Van Den Berg, G.; De Jong, L.; Benschop, H. *J. Am. Chem. Soc.* **1986**, *108*, 8290–8291.
(34) Millard, C. B.; Olson, M. A.; Carlacci, L.; Ordentlich, A.; Barak, D.; Shafferman, A.; Silman, I.; Sussman, J. L. Presented at the International Meeting on Cholinesterases, Perugia, Italy, Sept 26−30, 2004.
(35) Millard, C.; Koellner, G.; Ordentlich, A.; Shafferman, A.; Silman, I.; Sussman, J. L. *J. Am. Chem. Soc.* **1999**, *121*, 9883–9884.
(36) Shafferman, A.; Ordentlich, A.; Barak, D.; Stein, D.; Ariel, N.; Velan, B. *Biochem. J.* **1997**, *324*, 996–998 (Pt 3)

Glu335 and interactions with Phe398 that restrict its mobility (data not shown). The phosphoramidate moiety has to tilt toward His438Nϵ2 in order to promote formation of the salt bridge. There is also a significant reinforcement of the interactions between the phosphoryl oxygen and the oxyanion hole in the aged form of tabun−hBChE. This is likely related to an increase in electron density in the oxyanion hole oxygen linked to the delocalization of the new negative charge on the phosphorus O2-oxygen. Similar observations were made during the aging of soman−hBChE (Weik, M., personal communication) and echothiophate−hBChE.[10] These features, taken together, are thought to raise the activation energy needed for the dephosphylation reaction, thus rendering oxime-mediated reactivation virtually impossible after aging.

Interestingly, as a result of aging, the phosphoramidate tilts so that the dimethylamine moiety is less constrained and the two methyls point toward Trp231 to better fill in the acyl-binding pocket.

By contrast to hBChE, the catalytic histidine of AChEs (His447 in hAChE) is mobile. This was shown in NMR studies of the short strong hydrogen bond of aged TcAChE[37] and in crystal structure studies on non-aged VX−TcAChE.[35] It was suggested that this mobility was related to the lack of aromatic trapping.[38] Indeed, AChEs lack the aromatic residue equivalent to Phe398 in hBChE that provides stabilization for His438. A valine is found at the equivalent position in mAChE, hAChE, and TcAChE. The mobility of His447 is again illustrated in non-aged tabun−mAChE, as described by Ekstrom et al.[16] and reaffirmed in the present study. His447 and Phe338 shift in concert to avoid unfavorable contacts with the phosphoramidate moiety. Surprisingly, His447 adopts a continuum of conformations in the aged form. This was unexpected because the dealkylation and subsequent formation of a salt bridge normally releases the steric constraints on His447 and stabilizes the imidazolium into a well-defined conformation. The continuum of conformations could be due to the partial dealkylation, and to the coexistence of non-aged and aged conformations (Figure 8). The presence of an unknown ligand interfering with Tyr337 and indirectly with Phe338 might also contribute to the conformation disturbance of His447. Despite the conformational heterogeneity, the phosphoramidate moiety tips slightly toward His437 when the His occupies its usual triad position. This leads to formation of the salt bridge as observed in other aged AChE-OP conjugates.[9,35]

Nonaged cholinesterases inhibited by tabun are known to be resistant to most oxime reactivators.[6] It is acknowledged that oximes based on pyridinium aldoxime like HI-6 are too bulky to achieve a favorable orientation of the reactive group in the narrow active site of hAChE.[39−41] A smaller nucleophile capable of slipping in between the aromatic residues would be highly desirable to improve the efficiency of oxime reactivators. However, limited accessibility of the active site might not be the sole cause for the poor reactivation of tabun−ChE conjugates. The reactivation rate for tabun−hBChE is slow despite the fact that the active site is wide. This suggests that reactivation might be limited by the chemistry of the reaction. Partial delocalization of electron density from the nitrogen lone pair in the P−N bond on the phosphorus atom could reduce its electrophilicity, making it less susceptible to nucleophiles. Quantum mechanics/molecular mechanics (QM/MM) studies of the reactivation reaction based on tabun−mAChE and tabun−hBChE X-ray structures could clarify this point.

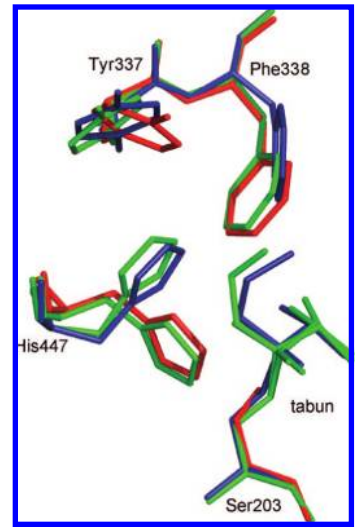

Figure 8. Superimposition of active sites of apo (red), non-aged (blue), and aged (green; two conformations, reflecting partial dealkylation of the tabun, are shown) tabun−mAChE conjugates. This figure highlights the conformational heterogeneity of His447, Tyr337, and Phe338.

Finally, the X-ray structures of tabun−ChEs provide a template on which to design mutants of human cholinesterases that can spontaneously and more efficiently reactivate from OP inhibition. G117H hBChE[42] is a model for such mutations, but more efficient variants are needed. The mutagenesis strategy based on computational design (QM/MM) that was successfully implemented for designing a mutant of hBChE with improved cocaine hydrolase activity[43] could be applied to the design of more active hBChE mutants capable of hydrolyzing OPs.

Efficient BChE-based catalytic bioscavengers would provide a great improvement in prophylaxis, decontamination, and treatment of organophosphate poisoning.

Acknowledgment. This work was supported by DGA grant 03co10-05/PEA 01 08 7 to P.M. and by DGA/PEA 08co501 and ANR-06-BLAN-0163 to F.N.

JA804941Z

(37) Massiah, M. A.; Viragh, C.; Reddy, P. M.; Kovach, I. M.; Johnson, J.; Rosenberry, T. L.; Mildvan, A. S. *Biochemistry* **2001**, *40*, 5682–5690.
(38) Kaplan, D.; Barak, D.; Ordentlich, A.; Kronman, C.; Velan, B.; Shafferman, A. *Biochemistry* **2004**, *43*, 3129–3136.
(39) Wong, L.; Radic, Z.; Bruggemann, R. J.; Hosea, N.; Berman, H. A.; Taylor, P. *Biochemistry* **2000**, *39*, 5750–5757.
(40) Kovarik, Z.; Radic, Z.; Berman, H. A.; Simeon-Rudolf, V.; Reiner, E.; Taylor, P. *Biochemistry* **2004**, *43*, 3222–3229.
(41) Luo, C.; Leader, H.; Radic, Z.; Maxwell, D. M.; Taylor, P.; Doctor, B. P.; Saxena, A. *Biochem. Pharmacol.* **2003**, *66*, 387–392.
(42) Millard, C. B.; Lockridge, O.; Broomfield, C. A. *Biochemistry* **1995**, *34*, 15925–15933.
(43) Pan, Y.; Gao, D.; Yang, W.; Cho, H.; Yang, G.; Tai, H. H.; Zhan, C. G. *Proc. Natl. Acad. Sci. U.S.A.* **2005**, *102*, 16656–16661.